

Left Ventricular Mechanics in Functional Ischemic Mitral Regurgitation in Acute Inferoposterior Myocardial Infarction

Zivile Valuckiene¹, M.D., Justas Ovsianas^{1,2}, M.D., Ruta Ablonskyte-Dudoniene¹, Ph.D., Vaida Mizariene¹, Ph.D., Karolina Melinyte¹, and Renaldas Jurkevicius¹ Ph.D.

¹Department of Cardiology, Lithuanian University of Health Sciences, Eiveniu 2, LT-50009, Kaunas, Lithuania; and ²Klinikum Gutersloh, Reckenberger Straße 19, 33332, Gutersloh, Germany

Ischemic mitral regurgitation (MR) is an established adverse prognostic factor after myocardial infarction (MI). Functional ischemic mitral regurgitation in acute phase of MI remains under-investigated due to its often transient and dynamic nature. We aimed to assess left ventricular (LV) mechanics by speckle-tracking echocardiography in acute inferoposterior MI and ischemic mitral regurgitation (MR). Methods: Sixty-nine patients with no structural cardiac valve abnormalities and first acute inferoposterior MI were prospectively enrolled into the study. Two-dimensional transthoracic echocardiography for regional myocardial function and valve assessment was performed within 48 hours of presentation after reperfusion therapy (percutaneous coronary intervention). Based on degree of MR, patients were divided into no significant MR (NMR) group (N = 34, with no or mild (grade 0–I) MR) and ischemic MR (IMR) group (N = 35, with grade ≥ 2 MR). Thirty-five age- and gender-matched healthy individuals served as a normal reference group. Offline 2D speckle tracking analysis was performed with GE EchoPAC software. Results: LV ejection fraction and longitudinal myocardial deformation parameters were significantly better in healthy subjects, but did not differ between both study groups. All circumferential myocardial deformation parameters were significantly worse in IMR group compared to healthy subjects and NMR group. Global, basal, and mid-ventricular radial strain was significantly lower in IMR group compared to both—healthy subjects and NMR group. Conclusion: Ischemic mitral regurgitation in acute inferoposterior MI is associated with worse radial and circumferential LV deformation parameters assessed by 2D speckle tracking echocardiography. (*Echocardiography* 2016;33:1131–1142)

Key words: speckle tracking echocardiography, ischemic mitral regurgitation

Ischemic mitral regurgitation (MR) is a recognized complication of myocardial infarction (MI). Multiple mechanisms are pathophysiologically involved: left ventricular (LV) contractile dysfunction and remodeling, tethering of the mitral valve leaflets with annular dilatation, and impaired mitral annular dynamics.¹ Although much is known about ischemic MR in remote phase, functional ischemic MR in acute phase of MI

remains under-investigated due to its often transient and dynamic nature in the presence of acute myocardial ischemia, relatively short acute MI period and rapid LV remodeling.

Speckle tracking echocardiography provides detailed and reproducible assessment of global and regional LV function, thus enhancing understanding of normal myocardial mechanics and alterations of myocardial deformation indices in the presence of various myocardial disorders.^{2–4} The aim of this study was to assess LV mechanics in acute inferoposterior MI with and without ischemic MR.

Materials and Methods:

Study Population:

Study population consisted of 69 patients treated for the first-ever inferoposterior acute MI at Hospital of Lithuanian University of Health Sciences Kaunas Clinics between January 2013 and June 2014, which were prospectively enrolled into the study. Ethical approval was

Funding Sources: There were no external sources of funding obtained for this study.

Address for correspondence and reprint requests: Zivile Valuckiene, M.D., Department of Cardiology, Lithuanian University of Health Sciences, Eiveniu St. 2, LT-50009 Kaunas, Lithuania. Fax: +370 37 331395; E-mail: z.valuckiene@gmail.com

This is an open access article under the terms of the Creative Commons Attribution-NonCommercial-NoDerivs License, which permits use and distribution in any medium, provided the original work is properly cited, the use is non-commercial and no modifications or adaptations are made.

obtained for the study, and all participants gave written informed consent prior to enrollment.

All patients with MI presented within 12 hours of symptom onset and were treated by primary or ad hoc percutaneous coronary intervention. Exclusion criteria were as follows: history of ischemic heart disease (any form of angina, previous MI, coronary artery bypass surgery, or occlusive/subocclusive lesions in nonculprit coronary arteries, suggestive of previous ischemic events), mechanical complications of myocardial infarction, suboptimal echocardiographic imaging quality, rhythm and conduction abnormalities (atrial fibrillation, atrioventricular node or His bundle branch block, implanted pacemaker), organic mitral valve disease, previously known mitral valve insufficiency, other left-sided valvular heart disease (including previous valvular heart surgery), other noncardiac disorders that may influence myocardial contractility (diabetes mellitus, renal insufficiency), and cardiogenic shock.

Acute MI was confirmed according to ESC recommendations of MI definition and guidelines based on clinical symptoms, electrocardiographic (ECG) findings, and cardiac enzyme abnormalities.⁵ Family history of IHD, cardiovascular risk factors, time of symptom onset, and current treatment were recorded using a standard questionnaire. Hypertension was defined as the presence of elevated systolic (>140 mmHg) and/or diastolic (>90 mmHg) blood pressure or current use of antihypertensive drugs. A patient was considered as a smoker if he was currently smoking or was a smoker in the past. Dyslipidemia was defined if any of the following criteria were present: serum total cholesterol ≥ 5.2 mmol/l, low-density lipoproteins >2.6 mmol/l, triglycerides ≥ 1.7 mmol/l, or current use of statin medication.⁶

Patients were consented and enrolled into the study after routine transthoracic echocardiogram, which has been performed within 48 hours of presentation and reperfusion therapy as routine investigation. If they agreed to participate, written informed consent was obtained and additional images were acquired for speckle tracking and mitral regurgitation analysis during the same examination. Thirty-four patients who met inclusion criteria and had competent or only trivially (grade I) incompetent mitral valve were enrolled into no or only mild MR (NMR) group. A matched number ($N = 35$) of patients with grade $>I$ MR were enrolled into ischemic MR (IMR) group. Due to multiple exclusions criteria, study patients were not enrolled in a consecutive manner.

Control Group:

Control group consisted of 35 healthy age-matched nonobese individuals with no history of ischemic heart disease or other non-cardiac disor-

ders that may affect myocardial contractility (arterial hypertension, renal failure, or diabetes mellitus). They all had normal electrocardiograms and no structural or functional cardiac abnormalities detectable by echocardiography. Control group participants were not on any form of medication (prescribed or over-the-counter).

Coronary Angiography Data Interpretation:

Coronary angiography data were analyzed and interpreted by one experienced interventional cardiologist.

Coronary dominance was defined according to the artery, which supplies the posterior descending artery (PDA) and labeled as right (if PDA originates from right coronary artery), left (if PDA originates from left circumflex coronary artery), or balanced (if PDA branches originate from both—right and left circumflex coronary arteries). Coronary blood flow was assessed by “Thrombolysis In Myocardial Infarction” (TIMI) grading (0—no antegrade flow, 1—weak contrast penetration beyond occlusion, 2—slow flow, 3—normal flow in the coronary artery).⁷ Collateral development to the culprit artery was quantified according to Rentrop classification.⁸

Echocardiography:

2D echocardiography was performed within 48 hours of presentation and reperfusion therapy (PCI) by one experienced physician-echocardiographer. Patients were imaged in the left lateral decubitus position using GE Vivid 7 echocardiography system (GE-Vingmed Ultrasound AS, Horten, Norway). Standard images were obtained using 3.5-MHz transducer in the parasternal (long- and short-axis views) and apical (four-, two-chamber, and long-axis) views. The frame rates of acquired images were between 82 and 95 frames/sec. Standard 2D and color Doppler data of at least three consecutive cardiac cycles, triggered to QRS complex, were saved in a cine loop format at a breath hold at shallow expiration.

2D echocardiography was used to assess conventional echocardiographic parameters. LV end-diastolic diameter (LVEDD), LV end-systolic diameter (LVESD), and left atrium (LA) diameters were measured from parasternal long-axis view (LVEDD at end-diastole, LVESD and LA diameters at end-systole). End-diastole was defined as the cardiac cycle time and frame when LV internal diameter was largest and end-systole as the frame when the LV cavity was smallest. LV dimensions were measured perpendicularly to LV long axis from the endocardial border of interventricular septum to the endocardial border of posterior LV wall immediately below the level of the mitral valve leaflet tips. LA anteroposterior diameter was measured from the endocardial border of

anterior LA wall to the endocardial border of posterior LA wall at the level of aortic valve perpendicularly to LA long axis.

LV ejection fraction (LVEF), LV end-diastolic volume (LVEDV), and LV end-systolic volume (LVESV) were automatically calculated by 2D biplane Simpson's method by manually tracing endocardial border of LV cavity in the largest (end-diastolic) and smallest (end-systolic) frames at the apical 4- and 2-chamber views. Myocardial mass (MM) was calculated by Devereux formula.⁹ Myocardial mass index (MMI) was calculated by dividing MM (g) by body surface area, BSA (m²).

Left ventricular regional function was quantified by 16-segment model.¹⁰ Each myocardial segment was scored individually based on myocardial thickening and endocardial motion: 1—normal/hyperkinetic, 2—hypokinetic/reduced thickening, 3—akinetic/absent thickening, 4—dyskinetic/aneurysmal. Total semiquantitative wall-motion score index (WMSI) was derived by dividing the global wall-motion score by the number of segments analyzed.

RV diameter was measured from apical 4-chamber view perpendicularly to the long RV axis at mid-ventricular level at end-diastole (cardiac cycle frame when RV internal diameter was largest).

Measurements of the Mitral Apparatus:

All measurements were obtained by one experienced echocardiographer from 2D echocardiographic views at end-systole, defined as the cardiac cycle frame where the LV cavity is smallest and mitral valve leaflets are closed. Mitral annular (MA) dimensions were obtained from apical long-axis (3-chamber) view (anteroposterior (AP) diameter) and apical bicommissural view (inter-commissural (IC) distance) when P1-A2-P3 mitral leaflet scallops are visualized, as the distance between opposite sites of leaflet insertion to the fibrotic annulus. MA area was calculated using the formula of an ellipse: $MAA = \pi * r_1 * r_2 / 4$, where r_1 and r_2 were AP and IC mitral annular dimensions, respectively.¹¹ Mitral leaflet tenting area was derived by manually tracing the triangular zone comprised by MA, valve leaflets, and the coaptation point from the apical 3-chamber view. Mitral leaflet tethering height was measured as the shortest perpendicular distance between the MA plane (reflected by the line connecting contralateral leaflet insertion points to the annulus) and the leaflet coaptation point at apical 3-chamber view. The posteromedial papillary muscle (PMPM) displacement was quantified as the distance between the PMPM tip and contralateral anterior mitral annulus (the site of anterior leaflet

insertion) in the apical 3-chamber view. Interpapillary muscle distance (IPMD) was measured between the endocardial borders of the papillary muscle heads from parasternal short-axis mid-ventricular level view with both papillary muscles visible in cross section. All mitral apparatus measurements were indexed to individual BSA to obtain standardized values.

Quantification of MR:

Mitral regurgitation was quantified by standard PISA method according to the recommendations provided by European Association of Cardiovascular Imaging¹² and reported as none (grade 0), mild (grade I, regurgitant orifice area (ROA) <0.2 cm²), moderate (grade II, ROA 0.2–0.3 cm²), or severe (grade III–IV, ROA ≥0.3 cm² or ≥0.4 cm², respectively). Based on mitral regurgitation degree, all study patients were divided into two subgroups: no significant mitral regurgitation group (NMR) (no or mild mitral regurgitation, grade 0–I) and ischemic mitral regurgitation (IMR) group (grade II–IV) (Fig. 1).

Myocardial deformation analysis:

2D speckle tracking imaging analysis was performed off line with GE EchoPAC software. For speckle tracking imaging analysis, end-systole was defined as the time of aortic valve closure from pulsed-wave Doppler tracing over LV outflow tract. All study population subjects had optimal segmental tracking in all LV segments and regions.

The following myocardial deformation parameters were evaluated:

Longitudinal: global and global peak systolic strain (GLS and GLPSS), basal and basal peak systolic strain (BLS and BLPSS), mean and peak mid-ventricular systolic strain (MLS and MLPSS), apical and apical peak systolic strain (ALS and ALPSS), and global peak systolic strain rate (GLPSSr);

Circumferential: global and global peak systolic strain (GCS and GCPSS), basal and basal peak systolic strain (BCS and BCPSS), mid-ventricular and mid-ventricular peak systolic strain (MCS and MCPSS), apical and apical peak systolic strain (ACS and ACPSS), and global, basal, mid-ventricular, and apical peak systolic strain rate (GCPSSr, BCPSSr, MCPSSr, and ACPSSr);

Radial: global and global peak systolic strain (GRS and GRPSS), basal and basal peak systolic strain (BRS and BRPSS), mid-ventricular and mid-ventricular peak systolic strain (MRS and MRPSS), apical and apical peak systolic strain (ARS and ARPSS), and global, basal, mid-ventricular, and apical peak systolic strain rate (GRPSSr, BRPSSr, MRPSSr, and ARPSSr);

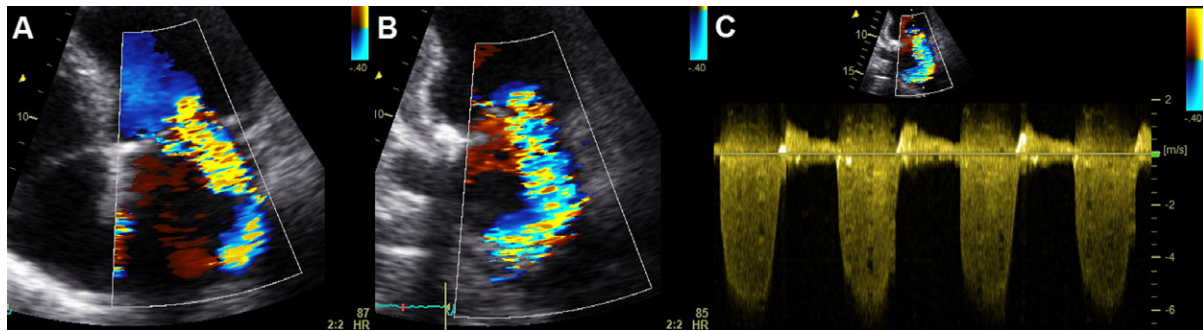


Figure 1. 2D transthoracic echocardiographic image with color flow (CF) and continuous-wave (CW) Doppler of a patient with an inferior myocardial infarction and severe functional ischemic mitral regurgitation (MR). **A.** Apical four-chamber view demonstrating severe laterally directed functional MR jet with Coanda effect (“wall-hugging” appearance of the regurgitant flow resulting from jet dispersion along adjacent left atrial (LA) wall). Due to Coanda-like effect eccentric regurgitant, MR jets are often underestimated based solely on CF Doppler methods. Proximal isovelocity surface area (PISA) method is a more reliable quantitative tool recommended for grading severity of MR. **B.** Apical two-chamber view at the same aliasing velocity (Nyquist limit 40 cm/sec) illustrating a hemispheric PISA radius of 6.5 mm and a large central MR jet reaching the posterior LA wall. Basal inferior left ventricular myocardial segment appears bulging and echo-intense and corresponds to the infarct region. **C.** CW Doppler of MR jet allows quantification of the effective regurgitant orifice area (EROA = 0.32 cm²) and regurgitant volume (RV = 48 mL). Dense appearance of CW Doppler signal is a qualitative indicator of severe MR.

Peak systolic strain was defined as the maximal strain value during the ejection phase (between the beginning of the QRS complex and the aortic valve closure reference time points): peak negative deflection for longitudinal and circumferential deformations (myocardial shortening), and peak positive deflection for radial deformation (myocardial thickening). Peak systolic strain rate was defined as the maximal strain rate value during ejection phase depending on the plane of myocardial deformation measurement: peak negative deflection for longitudinal and circumferential planes, and maximal positive deflection for radial plane. Global LV strain values were derived from averaged peak systolic strain measures using semiautomated software from 3 apical views: 4-chamber, 2-chamber, and apical long-axis views. Strain rate values represent change in strain over time (s⁻¹) and were measured automatically.

LV twist (degrees, °) was estimated as the difference between maximal apical and basal rotation parameters. To standardize the location from which basal and apical short-axis views were obtained, the basal short-axis plane was obtained just below the mitral valve annulus, where the LV myocardium appears in the scanning plane throughout the cardiac cycle and the apical short-axis plane was obtained just above the apex, where the LV cavity is visualized throughout the cardiac cycle.

Statistical Analysis:

Continuous variables were expressed as means ± standard deviations (SD). Continuous variables were assessed using the unpaired Stu-

dent’s t-test and Mann–Whitney U-test, as appropriate. Categorical variables are presented as absolute numbers and percentages and were compared using Chi-square test. A P value <0.05 was considered statistically significant.

The Kolmogorov–Smirnov test was used to detect the normality of distribution of the data. The Student’s t-test was used to compare normally distributed variables, and Mann–Whitney U-test was used for abnormally distributed variables among groups. Chi-square test was used for comparison of categorical variables.

Linear logistic regression analysis was used to determine whether myocardial deformation parameters predict PISA radius in ischemic mitral regurgitation. First, for selection of myocardial deformation parameters that might independently predict ischemic MR, univariate analysis was performed. Univariate analysis was followed by forward stepwise multivariate linear regression: the variables with a P value <0.05 in the univariate analysis were entered into the model and those with P > 0.1 were removed; standardized coefficients (β) and 95% confidence intervals (CI) were obtained.

Pearson’s correlation coefficient (r) was used to evaluate correlations between PISA radius and myocardial deformation parameters assessed by speckle tracking echocardiography; |r| ≥ 0.4 was interpreted to show a substantial correlation.

Intra-observer variability was evaluated for the measurements of systolic longitudinal, circumferential, and radial strains in 15 randomly selected cases. Intra-class correlation coefficients (ICC) and Bland–Altman plot diagrams were used for the evaluation.

TABLE I
General Demographic and Echocardiographic Characteristics of the Study Groups

	Control Group (A) n = 35	NMR Group (B) n = 34	IMR Group (C) n = 35	P-Value		
				A vs B	A vs C	B vs C
Age, years	57.3 ± 6.1	60.38 ± 11.36	61.86 ± 12.02	0.254	0.08	0.7
Males, n (%)	21 (60.0)	27 (79.4)	19 (54.3)	0.082	0.632	0.03
BMI, kg/m ²	26.6 ± 3.2	28.0 ± 3.6	28.4 ± 4.7	0.075	0.152	1.0
Arterial hypertension, n (%)	0 (0)	17 (50.0)	24 (68.6)	0.009	<0.001	0.1
Dyslipidemia, n (%)	13 (37.1)	23 (67.6)	29 (82.9)	0.012	<0.001	0.1
Smoking, n (%)	10 (28.6)	24 (70.6)	20 (57.1)	0.001	0.016	0.2
Echocardiographic parameters						
LVEF, %	59.8 ± 6.8	51.6 ± 7.2	51.5 ± 9.2	<0.001	<0.001	1.0
ESD, mm	48.4 ± 6.1	50.5 ± 5.8	52.3 ± 5.3	0.113	0.001	0.3
ESDi, mm/m ²	25.4 ± 2.7	25.8 ± 2.3	27.3 ± 3.0	0.728	0.028	0.03
LVESD, mm	33.4 ± 5.2	36.7 ± 6.7	38.6 ± 6.0	0.360	<0.001	0.3
LVESDi, mm/m ²	17.5 ± 2.5	18.7 ± 3.0	20.2 ± 3.4	0.105	0.001	0.1
LVEDV, mm ³	104.0 ± 26.8	109.2 ± 28.4	109.2 ± 28.4	0.158	0.381	0.8
LVEDVi, mm ³ /m ²	52.3 ± 10.3	55.2 ± 11.5	55.8 ± 15.1	0.343	0.369	1.0
LVESV, mm ³	40.7 ± 15.6	53.6 ± 17.9	52.9 ± 24.4	0.001	0.02	0.6
LVESVi, mm ³ /m ²	21.1 ± 6.3	27.0 ± 7.6	27.4 ± 11.8	0.001	0.003	0.8
MMI, g/m ²	70.5 ± 17.7	103.9 ± 22.3	111.2 ± 28.8	<0.001	<0.001	0.3
LA, mm	33.0 ± 5.0	38 ± 4.7	37.9 ± 4.4	<0.001	<0.001	1.0
LAi, mm/m ²	17.4 ± 2.6	19.4 ± 2.2	19.8 ± 2.5	0.001	<0.001	0.5
Total WMS	16.0 ± 0.0	21.5 ± 2.6	22.3 ± 3.5	<0.001	<0.001	0.4
Inferior WMS	3.0 ± 0.0	5.7 ± 1.3	6.1 ± 1.4	<0.001	<0.001	0.3
Inferoseptal WMS	3.0 ± 0.0	3.9 ± 1.1	3.9 ± 1.5	<0.001	<0.001	0.9
Posterior WMS	3.0 ± 0.0	3.9 ± 1.0	4.0 ± 1.6	<0.001	<0.001	0.8
Lateral WMS	3.0 ± 0.0	3.0 ± 0.3	3.1 ± 0.4	0.1	0.1	0.4
WMSI	1.0 ± 0.0	1.3 ± 0.2	1.4 ± 0.2	<0.001	<0.001	0.4
Mitral apparatus characteristics						
MAA, mm ²	594.6 ± 117.2	750.4 ± 156.9	889.0 ± 246.0	0.002	<0.001	0.006
MAAi, mm ² /m ²	313.1 ± 62.0	382.9 ± 74.1	466.2 ± 131.5	0.008	<0.001	0.001
MA APd, mm	23.9 ± 3.2	29.2 ± 3.9	31.5 ± 5.0	<0.001	<0.001	0.1
MA APdi, mm/m ²	12.6 ± 2.0	14.9 ± 2.0	16.6 ± 3.3	0.001	<0.001	0.03
MA ICd, mm	31.4 ± 3.2	32.5 ± 3.7	35.4 ± 5.3	0.9	0.001	0.02
MA ICdi, mm/m ²	16.5 ± 1.7	16.6 ± 2.0	18.5 ± 3.1	1.0	0.003	0.005
Tenting area, mm ²	121.5 ± 30.2	143.7 ± 59.9	167.1 ± 63.5	0.3	0.002	0.2
Tenting area index, mm ² /m ²	63.8 ± 15.2	73.2 ± 29.0	87.5 ± 34.4	0.5	0.001	0.1
Tethering height, mm	4.7 ± 1.2	6.8 ± 2.0	7.9 ± 2.2	<0.001	<0.001	0.06
Tethering height index, mm/m ²	2.4 ± 0.6	3.4 ± 0.9	4.1 ± 1.1	<0.001	<0.001	0.02
PMPM displacement, mm	36.2 ± 4.7	39.5 ± 5.6	43.0 ± 4.8	0.02	<0.001	0.02
PMPM displacement index, mm/m ²	19.0 ± 2.1	20.3 ± 3.4	22.5 ± 3.2	0.2	<0.001	0.007
IPMD, mm	10.1 ± 2.0	12.8 ± 2.8	14.5 ± 3.5	0.001	<0.001	0.048
IPMDi, mm/m ²	5.3 ± 1.2	6.5 ± 1.4	7.6 ± 1.9	0.006	<0.001	0.02

NMR = no significant mitral regurgitation (grade 0–1) group; IMR = ischemic mitral regurgitation group; BMI = body mass index; LVEF = left ventricular ejection fraction; ESD = left ventricular end-diastolic diameter; LVESD = left ventricular end-systolic diameter; LVEDV = left ventricular end-diastolic volume; LVESV = left ventricular end-systolic volume; MMI = myocardial mass index; LA = left atrial diameter in systole; LAi = left atrial diameter index; MAAi = mitral annular area index; MA = mitral annulus; APd = anteroposterior diameter; APdi = anteroposterior diameter index; ICd = inter-commissural diameter; ICdi = inter-commissural diameter index; PMPM = posteromedial papillary muscle; IPMD = inter-papillary muscle distance; IPMDi = inter-papillary muscle distance index.

All statistical analyses were performed using Software Package for Social Sciences (SPSS) version 21.0 (SPSS, Chicago, IL, USA).

Results:

General demographic and conventional echocardiographic characteristics of all study participants are summarized in Table I.

All the study groups contained participants of similar age and BMI. Patients with MI had more ischemic heart disease risk factors (arterial hypertension, dyslipidemia, and smoking history) as compared to the control group. Patients with significant mitral regurgitation (IMR group) were more often females compared to patients with no or only mild MR (NMR group).

Control group population had higher LVBEF, lower LVESV, LVESV index (LVESVi), MMI, LA diameter, and LA index (LAI). Majority of conventional echocardiographic parameters were similar in IMR and NMR groups, except for LVEDDi, which was higher in IMR group. Some other echocardiographic dimensions (LVEDD and LVEDD index (LVEDDi), LVEDV index (LVEDVi), LVESD index (LVESDi) were higher only in IMR group as compared to the control subjects. LV wall-motion abnormalities were similar in both study groups and were not present in control subjects.

Characteristics of mitral apparatus are presented in Table I. Both study groups had significantly larger MAA, greater MA AP diameter index, and tethering height compared to control group. These parameters were also greater in IMR than in NMR group. MA IC distance was similar between control and NMR groups, however significantly increased in IMR group. Statistically significant difference in mitral valve tenting area was observed only between control and IMR groups. IPMD was increased in both groups of patients with MI and was greater in IMR group compared with NMR group. PMPM displacement was insignificant in NMR group compared to control group. In the meantime, IMR group had significantly increased PMPM-anterior MA distance compared to healthy subjects and patients with inferoposterior MI without significant MR (NMR group).

Clinical and angiographic characteristics of study patients with myocardial infarction are summarized and compared in Table II.

NMR and IMR group patients had similar distribution of timing from symptom onset to reperfusion therapy. IMR patients were more often found to have culprit lesion in LCx artery with no antegrade flow (TIMI flow grade 0) on initial coronary angiogram. NMR group more often had RCA being the culprit artery with preserved antegrade flow in MI region (TIMI flow grade 3). TIMI flow after PCI procedure was similar in both groups. Patients in IMR group had better developed collaterals compared to NMR group. Both groups did not differ in regard to PCI success (TIMI flow in the culprit artery after PCI).

2D speckle tracking myocardial deformation analysis results are depicted in Figures 2–9.

Almost all longitudinal myocardial deformation parameters (except for ALS and ALPSS, which were similar in NMR group and healthy subjects) were significantly better in healthy subjects as compared to the patients with MI. NMR and IMR groups did not differ in regard to longitudinal LV strains (Fig. 2). Figure 3 illustrates 2D longitudinal myocardial strain patterns of a healthy subject (2A) and selected patients from

TABLE II

Clinical and Angiographic Characteristics of Myocardial Infarction Groups

	NMR Group n = 34	IMR Group n = 35	P
Time from symptom onset to reperfusion			
≤4 h	16 (47.1)	10 (28.6)	0.116
4–8 h	9 (26.5)	10 (28.6)	0.846
8–12 h	9 (26.5)	15 (42.9)	0.156
Culprit lesion, n (%)			
RCA	31 (91.2)	22 (62.9)	0.006
LCx	3 (8.8)	13 (37.1)	0.006
TIMI flow before PCI			
0	14 (41.2)	23 (67.6)	0.043
1	2 (5.9)	1 (2.9)	0.541
2	7 (20.6)	6 (17.6)	0.716
3	11 (32.4)	3 (8.8)	0.015
TIMI flow after PCI			
0	0 (0)	3 (8.8)	0.083
1	1 (2.9)	1 (2.9)	0.984
2	3 (8.8)	2 (5.9)	0.621
3	30 (88.2)	28 (82.4)	0.354
Collateral flow			
0	25 (73.5)	16 (45.7)	0.02
1	7 (20.6)	4 (11.4)	0.302
2	2 (5.9)	15 (40)	<0.001

NMR = no significant mitral regurgitation (grade 0–1) group; IMR = ischemic mitral regurgitation group; RCA = right coronary artery; LCx = left circumflex coronary artery; TIMI = Thrombolysis in Myocardial Infarction coronary flow grade; PCI = percutaneous coronary intervention.

different study groups (3B and 3C) derived from apical 2-chamber view.

Global, basal, and mid-ventricular circumferential deformation parameters (GCS, GCPSS, BCS, BCPSS, MCS, and MCPSS) in control group had significantly higher values compared with other study groups. Apical circumferential myocardial deformation (ACS and ACPSS) was similar between control and NMR groups, but lower in IMR group. All circumferential deformation parameters were significantly lower in IMR group compared with NMR group (Fig. 4). Figure 5 illustrates 2D circumferential myocardial strain patterns of a healthy subject (5A) and selected patients from both study groups (5B and 5C) derived from parasternal short-axis view in the mid-ventricular level of LV.

Healthy subjects and NMR group patients were similar regarding all radial myocardial deformation parameters. Global, basal, and mid-ventricular radial strains (GRS, GRPSS, BRS, BRPSS, MRS, and MRPSS) were significantly lower in IMR patients as compared to both—NMR and control groups. There was no statistically significant difference in apical radial strain values among all

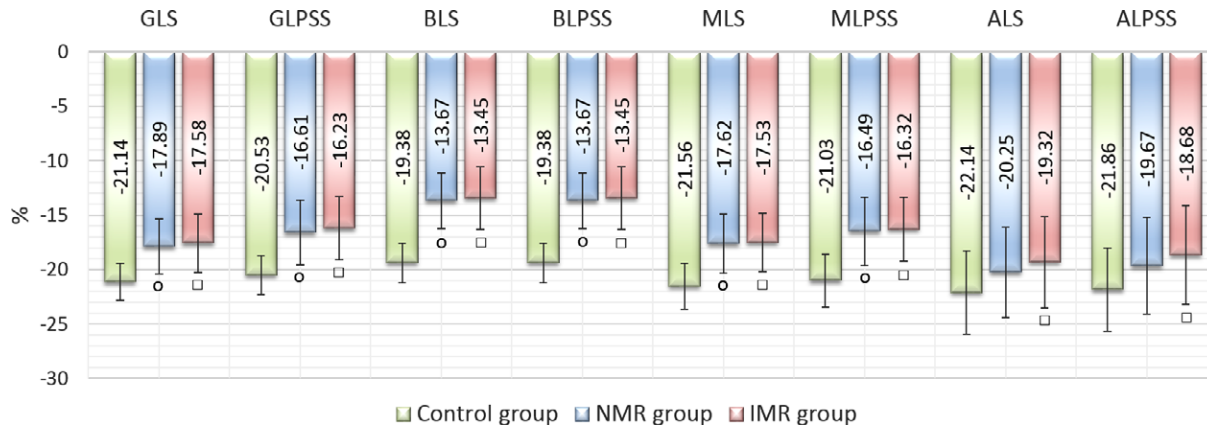


Figure 2. Longitudinal left ventricular myocardial deformation parameters. NMR = no significant mitral regurgitation (grade 0–1) group; IMR = ischemic mitral regurgitation group; GLS = global longitudinal strain; GLPSS = global longitudinal peak systolic strain; BLS = basal longitudinal strain; BLPSS = basal longitudinal peak systolic strain; MLS = mid-ventricular longitudinal strain; MLPSS = mid-ventricular longitudinal peak systolic strain; ALS = apical longitudinal strain; ALPSS = apical longitudinal peak systolic strain. ○—NMR versus Control group P < 0.05; □—IMR versus Control group P < 0.05.

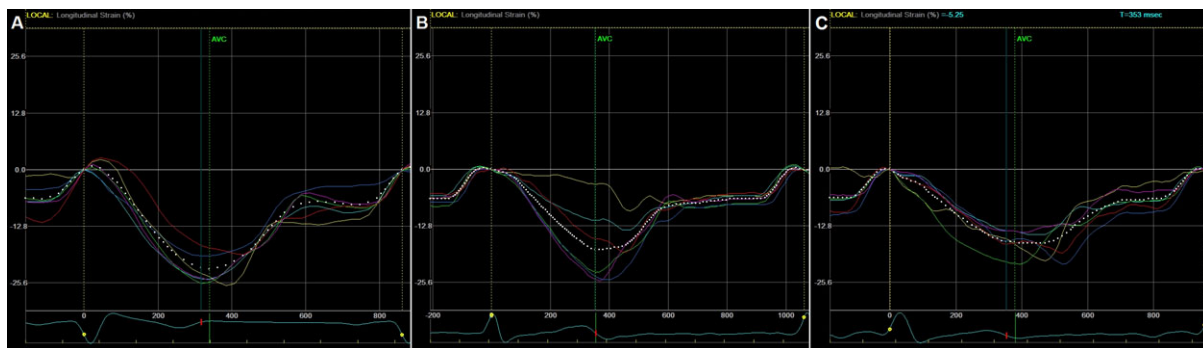


Figure 3. 2D longitudinal myocardial deformation strain patterns of the left ventricle (LV) derived from apical 2-chamber view. **A.** Healthy subject (control group). Color coding represents different segments of LV (yellow—basal inferior, light blue—mid-inferior basal, green—apical inferior, purple—anterior apical, dark blue—mid-anterior, red—basal anterior). Homogeneous onset and peak negative longitudinal strain pattern represents uniform myocardial contraction and shortening in all regions. **B.** Patient with inferior myocardial infarction (MI) and no mitral regurgitation (NMR group). Top yellow and blue lines represent basal and mid-inferior LV wall segments that have markedly lower systolic strain values (reduced systolic shortening). Late postsystolic contraction of these segments is observed as peak negative values occurring after aortic valve closure (AVC, marked as the green vertical line). **C.** Patient with inferoposterior MI and severe functional ischemic mitral regurgitation (IMR group). The strain curves show synchronous contraction, but lower values. The white dotted line represents average strain, which is lower if compared to a healthy subject or similar patient without MR.

study groups (Fig. 6). Illustrative examples of radial strain patterns in different study groups are depicted in Figure 7.

Distribution of LV strain rate patterns among the study groups is illustrated in Figure 8. GLPSSr was better in control, and similar between the study groups. GCPSSr, MCPSSr, ACPSSr, GRPSSr, BRPSSr, MRPSSr, and ARPSSr were similar between control and NMR groups and worse in IMR group. There was no significant difference in BCPSSr among the groups.

Both groups of patients with MI had worse basal LV rotational parameters compared to con-

control group. Apical rotation was similar in all three groups. LV twist was better in healthy subjects than in IMR group, but did not differ between control–NMR and NMR–IMR groups (Fig. 9).

GCS, GCPSS, GRS, and GRPSS had weak but significant correlations with PISA radius of MR (Table III). Longitudinal deformation parameters did not correlate to the grade of MR (PISA radius).

Table IV presents results of linear logistic regression analysis with PISA radius as dependent variable and myocardial deformation parameters as independent variables. Of all myocardial deformation parameters GRPSSr, MCS and MCPSS

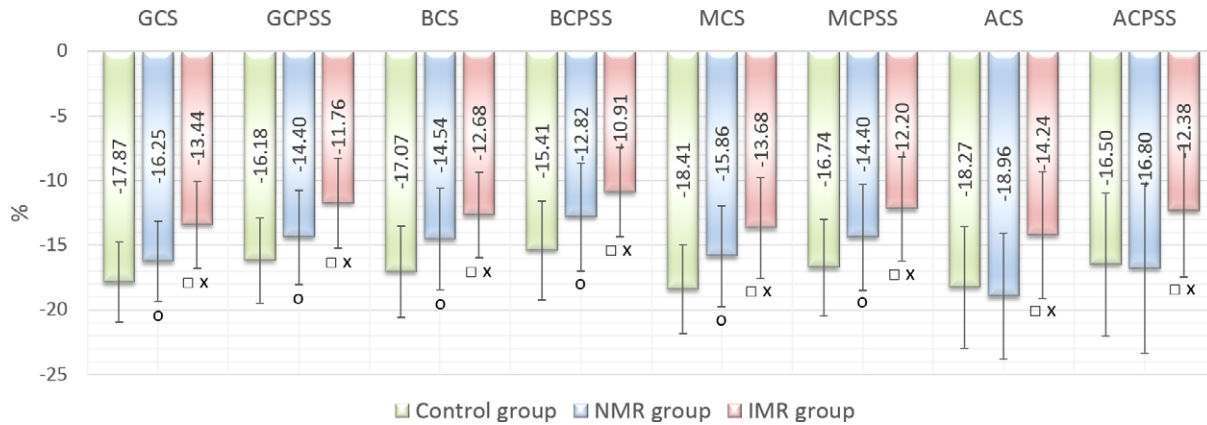


Figure 4. Circumferential left ventricular myocardial deformation parameters. NMR = no significant mitral regurgitation (grade 0–1) group; IMR = ischemic mitral regurgitation group; GCS = global circumferential strain; GCPSS = global circumferential peak systolic strain; BCS = basal circumferential strain; BCPSS = basal circumferential peak systolic strain; MCS = mid-ventricular circumferential strain; MCPSS = mid-ventricular circumferential peak systolic strain; ACS = apical circumferential strain; ACPSS = apical circumferential peak systolic strain. o—NMR versus Control group $P < 0.05$; □—IMR versus Control group $P < 0.05$; x—IMR versus NMR group $P < 0.05$.

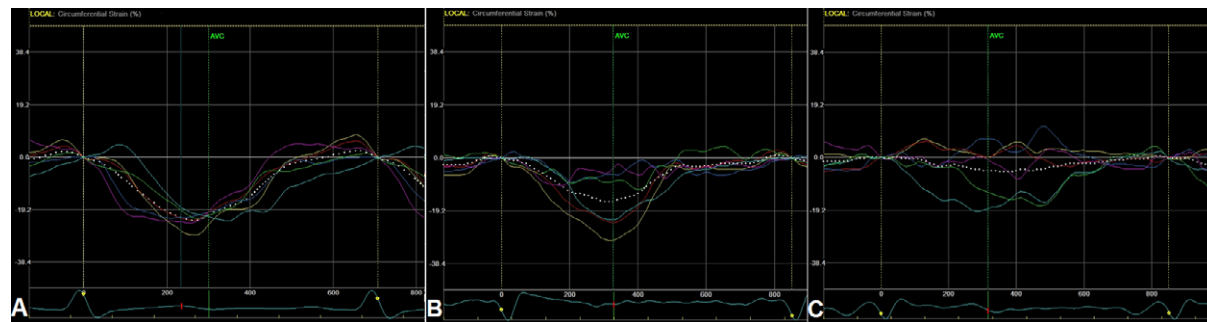


Figure 5. 2D circumferential myocardial strain patterns of the left ventricle (LV) derived from parasternal short-axis view at mid-ventricular level. **A.** Healthy subject (control group). Strain within each LV segment is color-coded and plotted over time (yellow—anteroseptal, light blue—anterior, green—lateral, purple—posterior, dark blue—inferior, red—(infero)septal). Circumferential strain has negative values, which reflect shortening of the myocardial fibers during inward motion resulting from wall thickening. **B.** Patient with inferoposterior myocardial infarction and no mitral regurgitation (NMR group). Segmental circumferential strain curves illustrate attenuated strain in inferior, posterior, and lateral LV regions (dark blue, purple, and green lines). This patient had a culprit infarct-related lesion in left circumflex coronary artery (LCx). Interestingly, there were no detectable wall-motion abnormalities in the lateral LV region on 2D imaging; however, circumferential strain abnormalities corresponding to the supplied LCx region were detectable by speckle tracking echocardiography. **C.** Patient with inferoposterior MI and severe functional ischemic mitral regurgitation (IMR group). The circumferential strain pattern is asynchronous and reflects severe myocardial dysfunction in inferior, posterior, and septal regions. The patient had culprit lesion in a dominant right coronary artery (RCA), giving rise to large posterior descending and posterolateral branches. RCA is known to provide septal perforators that supply inferior part of the interventricular septum; therefore, strain abnormalities (red line) in this part of LV are expected. Interesting to note that circumferential strain in adjacent anterior part of the septum (yellow line) is also greatly disturbed. It may be attributable to (1) overall integrity of the interventricular septum and involvement in the infarct zone, (2) individual anatomic variations of coronary perfusion, or (3) residual consequences of coronary steal phenomenon to the infarct region through septal collaterals from left anterior descending coronary artery.

were found to be the most significant predictors of ischemic mitral regurgitation.

Intra-Observer Variability:

Two-way random-effects model for absolute agreement showed strong intra-observer correlations for systolic longitudinal strain (ICC, 0.87;

95% confidence interval, 0.72–0.92), systolic circumferential strain (ICC, 0.91; 95% confidence interval 0.75–0.94), and systolic radial strain (ICC 0.94; 95% confidence interval, 0.88–0.97) measurements.

Intra-observer variation in Bland–Altman analysis were best for longitudinal strain measurements

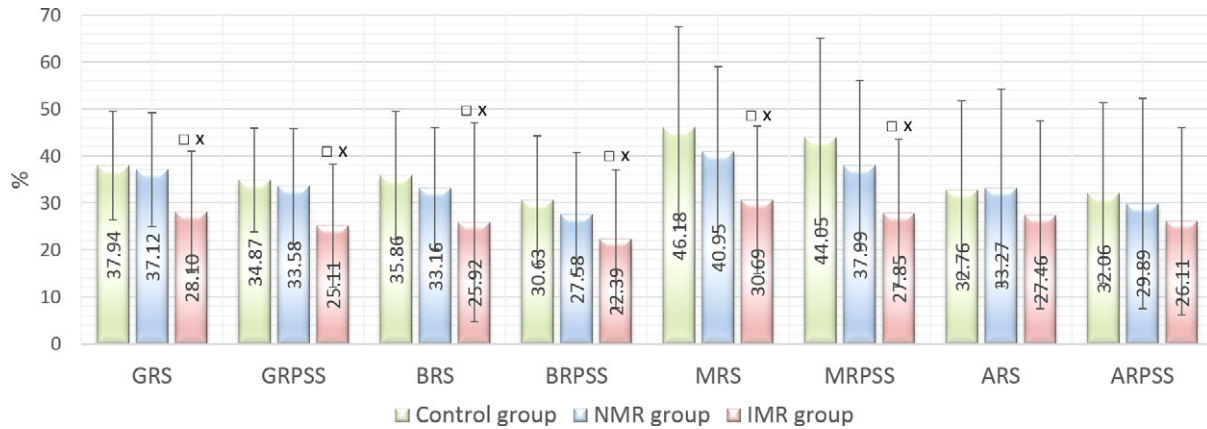


Figure 6. Radial left ventricular myocardial deformation parameters. NMR = no significant mitral regurgitation (grade 0–1) group; IMR = ischemic mitral regurgitation group; GRS = global radial strain; GRPSS = global radial peak systolic strain; BRS = basal radial strain; BRPSS = basal radial peak systolic strain; MRS = mid-ventricular radial strain; MRPSS = mid-ventricular radial peak systolic strain; ARS = apical radial strain; ARPSS = apical radial peak systolic strain. □—IMR versus Control group $P < 0.05$; x—IMR versus NMR group $P < 0.05$.



Figure 7. 2D radial myocardial deformation strain patterns derived from parasternal short-axis view at basal left ventricular (LV) level. **A.** Healthy subject (control group). The colored lines represent radial strain values of regional myocardial segments throughout the cardiac cycle (yellow—anteroseptal, light blue—anterior, green—lateral, purple—posterior, dark blue—inferior, red—infero)septal). Contraction is uniform and synchronous in all LV regions. Radial strain values are positive and reflect myocardial thickening. **B.** Patient with inferior myocardial infarction (MI) and no mitral regurgitation (NMR group). The radial strain pattern is preserved and peaks at the time of aortic valve closure (AVC). Peak strain values are lower if compared to a healthy subject. **C.** Patient with inferoposterior MI and severe functional ischemic mitral regurgitation (IMR group). Radial strain (myocardial thickening) is decreased in all segments, especially posterior, inferior, and septal regions (purple, dark blue, red, and yellow lines). Basal LV radial contraction is delayed (reaches its peak after AVC).

(−3.6% to +2.3%) and worst for radial strain measurements (−12.7% to +11.8%).

Discussion:

Speckle tracking echocardiography (STE) is advantageous compared to conventional echocardiographic determinants of LV systolic function (EF, wall-motion score) as is not influenced by tethering of adjacent myocardial segments, ultrasound beam alignment, and allows assessment of cardiac mechanics in all spatial planes: longitudinal, circumferential, and radial.^{2,13,14} Understanding alterations of myocardial contractility in various myocardial disorders may have important clinical and prog-

nostic implications.^{15,16} Functional ischemic mitral regurgitation in inferoposterior myocardial infarction is predominately predisposed by impaired regional LV contractility resulting in tethering and systolic restriction of posterior mitral valve leaflet, thus impeding mitral valve closure.^{17,18} This study has illustratively depicted changes in mitral anatomy resulting from inferoposterior MI, which are more exaggerated in the presence of ischemic MR: increased MAA and dimensions, mitral valve tenting, and subvalvular apparatus displacement. The aforementioned findings have been extensively described and discussed in a variety of published literature.^{1,19,20}

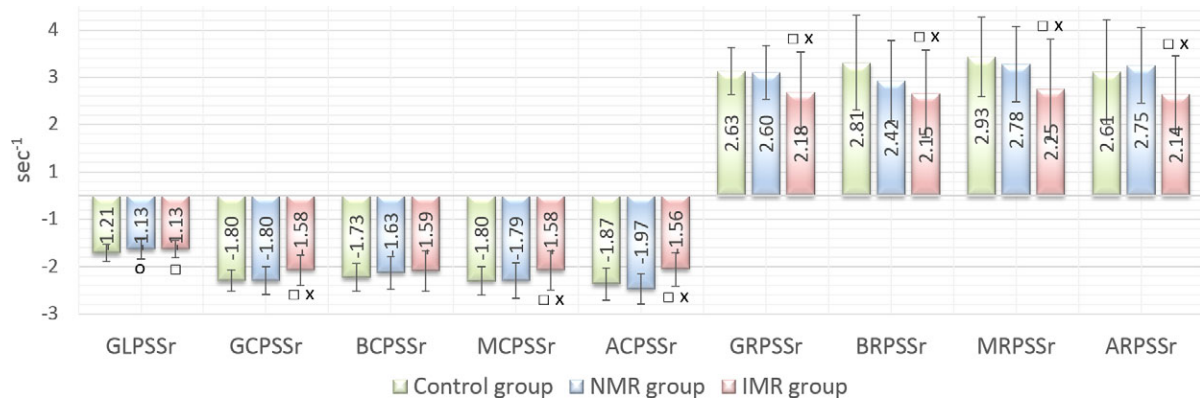


Figure 8. Left ventricular strain rate parameters. NMR = no significant mitral regurgitation (grade 0–1) group; IMR = ischemic mitral regurgitation group; GLPSSr = global longitudinal peak systolic strain rate; GCPSSr = global circumferential peak systolic strain rate; BCPSSr = basal circumferential peak systolic strain rate; MCPSSr = mid-ventricular circumferential peak systolic strain rate; ACPSSr = apical circumferential peak systolic strain rate; GRPSSr = global radial peak systolic strain rate; BRPSSr = basal radial peak systolic strain rate; MRPSSr = mid-ventricular radial peak systolic strain rate; ARPSSr = apical radial peak systolic strain rate. o—NMR versus Control group $P < 0.05$; □—IMR versus Control group $P < 0.05$; x—IMR versus NMR group $P < 0.05$.

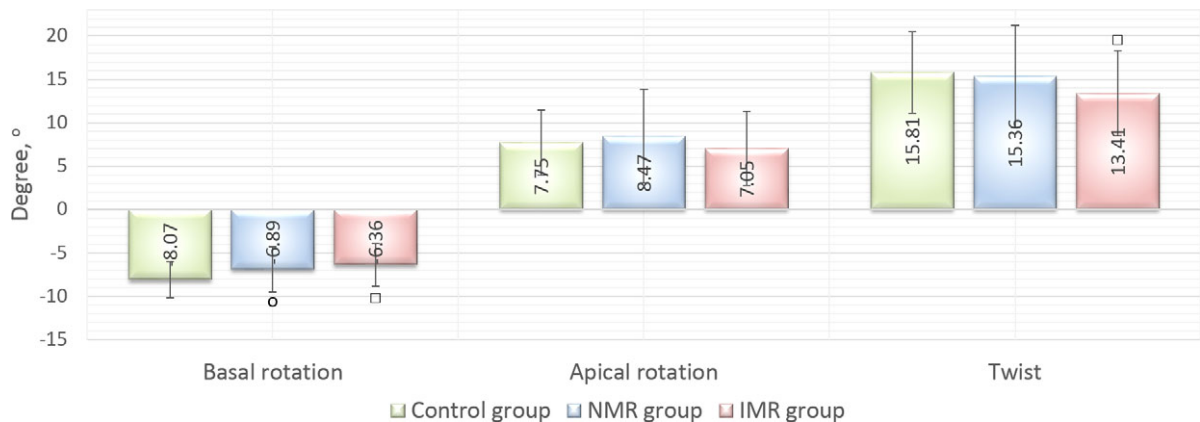


Figure 9. Left ventricular rotation parameters. NMR = no significant mitral regurgitation (grade 0–1) group; IMR = ischemic mitral regurgitation group. o—NMR versus Control group $P < 0.05$; □—IMR versus Control group $P < 0.05$.

TABLE III

Correlation of Myocardial Deformation Parameters and PISA Radius

	Correlation Coefficient	P Value
GLS	0.116	0.418
GLPSS	0.058	0.686
GCS	0.311	0.031
GCPSS	0.295	0.038
GRS	-0.318	0.014
GRPSS	-0.275	0.035

GLS = global longitudinal strain; GLPSS = global longitudinal peak systolic strain; GCS = global circumferential strain; GCPSS = global circumferential peak systolic strain; GRS = global radial strain; GRPSS = global radial peak systolic strain.

The major findings in our study were that the underlying myocardial dysfunction is attributable to impaired circumferential and radial myocardial

TABLE IV

Prognostic Myocardial Deformation Parameters of the Left Ventricle for Ischemic Mitral Regurgitation in Acute Inferoposterior Myocardial Infarction

Parameter	Standardized Coefficient (β)	95 CI for β	P
GRPSSr	-0.6	-1.2 – (-0.3)	0.002
MCS	-1.0	-0.7 – (-0.05)	0.026
MCPSS	0.9	0.003 – 0.6	0.048

GRPSSr = global radial peak systolic strain rate; MCS = mid-ventricular circumferential strain; MCPSS = mid-ventricular circumferential peak systolic strain; CI = confidence interval.

deformation in patients with ischemic MR in acute inferoposterior MI.

Subendocardial layer is the major contributor to longitudinal myocardial function as sustains

the greatest deformational changes during systole leading to higher oxygen demand and susceptibility to ischemia compared to other myocardial layers. Consequently, ischemia caused by acute myocardial infarction invariably affects the subendocardium and therefore longitudinal strain.¹³ Although longitudinal LV function (strain) is reduced in both study groups, it does not appear to be related to acute ischemic MR in acute inferoposterior MI.

Circumferential and radial deformation of myocardial fibers during systolic contraction (circumferential and radial strains) have also been demonstrated to be reduced in myocardial ischemia.²¹ Our study has demonstrated that circumferential strain is significantly reduced globally and regionally in patients with IMR compared to both control groups (healthy subjects and MI patients with no significant MR), and apparently has important role in genesis of ischemic MR. Circumferential systolic strain reflects shortening of myocardial fibers around LV cavity. Reduced circumferential strain is an indirect indicator of increased LV systolic sphericity, which may account for lateral traction of papillary muscles and subvalvular mitral apparatus. Also, lower circumferential strain values are associated with greater transmural scar formation.²²

Lower radial strain in patients with ischemic MR emphasizes the importance of radial myocardial thickening in basal and mid-ventricular regions in maintaining MV competence in acute inferoposterior MI and may lead to contractile papillary muscle dysfunction.

Circumferential and radial myocardial deformation parameters reveal important mechanistic determinants of ischemic MR in patients with acute inferoposterior MI with otherwise comparable conventional echocardiographic parameters (global EF, WMS) and longitudinal LV function. Above-mentioned findings once again prove superiority of STE over routine 2D echocardiographic measures (biplane EF or visual wall-motion assessment) in detecting left ventricular systolic dysfunction.^{2,13,21}

Myocardial infarction from histologic analysis is known to affect the myocardial layers to a different extent, resulting in either homogenous transmural ischemic injury or alterations limited to specific layers.²³ Higher extent of impaired LV mechanics suggests higher transmural injury of myocardial injury and dysfunction in IMR patients. Circumferential strain represents subepicardial layer; therefore, significant reduction in all circumferential strains supports this hypothesis. Studies involving cardiac magnetic resonance imaging would be beneficial to further confirm this finding.

Impaired basal rotational mechanics in inferoposterior MI has been described to be associated with increased MR.²⁴ Rotational motion of LV myocardium is essential to ensure normal function of a complex three-dimensional mitral apparatus structure (saddle-shaped annulus with inherent systolic contraction, etc.). Although our study has shown no difference in rotation between the patients with or without ischemic MR, this difference may become evident with LV remodeling over time. Further follow-up studies comparing LV mechanics in acute and chronic ischemic MR forms would reveal interesting mechanistic insights.

Time to reperfusion and preserved antegrade coronary flow in the culprit artery appear to be the most important angiographic factors in preventing ischemic MR. Although recent reports emphasize the importance of collateral supply in ischemic MR reduction, a considerable proportion of our study participants exhibited ischemic MR despite well-developed collateral circulation to occluded culprit artery territory. Recent findings revealed that collateral circulation compensates for antegrade flow reduction and relieves ischemia in stable coronary artery disease with chronic total occlusion in less than 5% of patients.²⁵ Likely collateral flow reserve is even less in acute ischemic event. Developed collateral circulation to the infarct zone in patients presenting with acute MI has also been reported to represent previously underlying silent ischemia and left ventricular remodeling, as well as indicates a higher likelihood for the patient to exhibit ischemic MR upon presentation.²⁶

Ischemic mitral regurgitation is strongly associated with adverse LV remodeling. Some patients are known to develop MR over time despite normal valve competence in acute MI period. As well, MR is known to resolve in some patients on longer-term follow-up; therefore, further studies are desirable to assess how LV mechanics contribute or predict remote MR progression or regression.

Study Limitations:

The study samples are small and may have been influenced by multiple exclusion criteria described at methodology part of this study, therefore preclude definitive conclusions.

IMR study group consisted of less males, who are known to have normally lower myocardial deformation values. However, this influence is negligible as myocardial deformation indices in other study groups consisting of more males were still proven superior to the IMR study group.

Conclusion:

Ischemic mitral regurgitation in acute phase of inferoposterior MI is associated with worse radial and circumferential LV deformation parameters assessed by 2D speckle tracking transthoracic echocardiography.

References

- Silbiger JJ: Mechanistic insights into ischemic mitral regurgitation: Echocardiographic and surgical implications. *J Am Soc Echocardiogr* 2011;24:707–719.
- Abdouch MC, Alencar AM, Mathias W Jr, et al: Cardiac mechanics evaluated by speckle tracking echocardiography. *Arq Bras Cardiol* 2014;102:403–412.
- Dalen H, Thorstensen A, Aase SA, et al: Segmental and global longitudinal strain and strain rate based on echocardiography of 1266 healthy individuals: The HUNT study in Norway. *Eur J Echocardiogr* 2010;11:176–183.
- Helle-Valle T, Crosby J, Edvardsen T, et al: New noninvasive method for assessment of left ventricular rotation: Speckle tracking echocardiography. *Circulation* 2005;112:3149–3156.
- Thygesen K, Alpert JS, Jaffe AS, et al: Third universal definition of myocardial infarction. *Eur Heart J* 2012;33:2551–2567.
- Catapano AL, Reiner Z, De Backer G, et al: ESC/EAS Guidelines for the management of dyslipidaemias. The Task Force for the management of dyslipidaemias of the European Society of Cardiology (ESC) and the European Atherosclerosis Society (EAS). *Atherosclerosis* 2011;217:3–46.
- The TIMI Study Group: The Thrombolysis in Myocardial Infarction (TIMI) trial. Phase I findings. *N Engl J Med* 1985;312:932–936.
- Rentrop KP, Cohen M, Blanke H, et al: Changes in collateral channel filling immediately after controlled coronary artery occlusion by an angioplasty balloon in human subjects. *J Am Coll Cardiol* 1985;5:587–592.
- Foppa M, Duncan BB, Rohde LEP: Echocardiography-based left ventricular mass estimation. How should we define hypertrophy? *Cardiovasc Ultrasound* 2005;3:17.
- Schiller NB, Shah PM, Crawford M, et al: Recommendations for quantitation of the left ventricle by two-dimensional echocardiography. American Society of Echocardiography Committee on Standards, Subcommittee on Quantitation of Two-Dimensional Echocardiograms. *J Am Soc Echocardiogr* 1989;2:358–367.
- Hyodo E, Iwata S, Tugcu A, et al: Accurate measurement of mitral annular area by using single and biplane linear measurements: Comparison of conventional methods with the three-dimensional planimetric method. *Eur Heart J Cardiovasc Imaging* 2012;13:605–611.
- Lancellotti P, Tribouilloy C, Hagendorff A, et al: Recommendations for the echocardiographic assessment of native valvular regurgitation: An executive summary from the European Association of Cardiovascular Imaging. *Eur Heart J Cardiovasc Imaging* 2013;14:611–644.
- Mizuguchi Y, Oishi Y, Miyoshi H, et al: The functional role of longitudinal, circumferential, and radial myocardial deformation for regulating the early impairment of left ventricular contraction and relaxation in patients with cardiovascular risk factors: A study with two-dimensional strain. *J Am Soc Echocardiogr* 2008;21:1138–1144.
- Onishi T, Saha SK, Delgado-Montero A, et al: Global longitudinal strain and global circumferential strain by speckle-tracking echocardiography and feature-tracking cardiac magnetic resonance imaging: Comparison with left ventricular ejection fraction. *J Am Soc Echocardiogr* 2015;28:587–596.
- Cong T, Sun Y, Shang Z, et al: Prognostic value of speckle tracking echocardiography in patients with ST-elevation myocardial infarction treated with late percutaneous intervention. *Echocardiography* 2015;32:1384–1391.
- Shehata M: Value of two-dimensional strain imaging in prediction of myocardial function recovery after percutaneous revascularization of infarct-related artery. *Echocardiography* 2015;32:630–637.
- Kumanohoso T, Otsuji Y, Yoshifuku S, et al: Mechanism of higher incidence of ischemic mitral regurgitation in patients with inferior myocardial infarction: Quantitative analysis of left ventricular and mitral valve geometry in 103 patients with prior myocardial infarction. *J Thorac Cardiovasc Surg* 2003;125:135–143.
- Anyanwu A, Rahmanian PB, Filsoofi F, et al: The pathophysiology of ischemic mitral regurgitation: Implications for surgical and percutaneous intervention. *J Intervent Cardiol* 2006;19:S78–S86.
- Meris A, Amigoni M, Verma A, et al: Mechanisms and predictors of mitral regurgitation after high-risk myocardial infarction. *J Am Soc Echocardiogr* 2012;25:535–542.
- Agricola E, Oppizzi M, Pisani M, et al: Ischemic mitral regurgitation: Mechanisms and echocardiographic classification. *Eur J Echocardiogr* 2008;9:207–221.
- Winter R, Jussla R, Nowak J, et al: Speckle tracking echocardiography is a sensitive tool for the detection of myocardial ischemia: A pilot study from the catheterization laboratory during percutaneous coronary intervention. *J Am Soc Echocardiogr* 2007;20:974–981.
- Chan J, Hanekom L, Wong C, et al: Differentiation of subendocardial and transmural infarction using two-dimensional strain rate imaging to assess short-axis and long-axis myocardial function. *J Am Coll Cardiol* 2006;48:2026–2033.
- Flameng W, Wouters L, Sergeant P, et al: Multivariate analysis of angiographic, histologic and electrocardiographic data in patients with coronary heart disease. *Circulation* 1984;70:7–17.
- Sanz J, Weinsaft JW: Ischemic mitral regurgitation: Is mitral valve physiology moving from global to local? *J Am Coll Cardiol* 2014;64:1880–1882.
- Traupe T, Gloekler S, Marchi SF, et al: Assessment of the human coronary collateral circulation. *Circulation* 2010;122:1210–1220.
- Valuckiene Z, Budrys P, Jurkevicius R: Predicting ischemic mitral regurgitation in patients with acute ST-elevation myocardial infarction: Does time to reperfusion really matter and what is the role of collateral circulation? *Int J Cardiol* 2015;203:667–671.